JOURNAL OF MATERIALS SCIENCE **39** (2004) 6467–6472

Formability of AA8011 aluminum alloy sheet in homogenized and unhomogenized conditions

M. AGHAIE-KHAFRI
Faculty of Mechanical Engineering, K.N. Toosi University of Technology, P.O. Box 16765-3381, Tehran, Iran
E-mail: maghaei@kntu.ac.ir

The present study examines the microstructure and formability of homogenized and unhomogenized AA8011 aluminum alloy sheets under uniaxial and biaxial deformation modes. The stretch formability of sheets has been characterized in terms of limit strains in forming limit diagrams (FLDs). The formability of the material is associated with combinations of strain hardening, strain-rate hardening and surface roughening which is developed during the plastic deformation of the material. The phenomenon of recrystallization and the effect of second phase particles has been investigated in cold rolled sheets. It appears that surface roughening which is in turn a result of the grain coarsening is more important in the homogenized materials annealed at high temperatures.

1. Introduction

Aluminum alloy AA8011 which is generally used for household foil is an attractive material due to the fact that it can provide a suitable combination of strength and ductility. The principal strengthening agents in AA8011 alloy are the Fe-Si constituent particles. These particles are capable of stabilizing a fine grain or subgrain structure which can develop interesting combinations of strength and ductility. However, most of the investigations carried out on the AA8011 aluminum sheets are concerned with the recrystallization and precipitation behavior of this material. Ney and Luiggi [1] have characterized a commercial AA8011 alloy by studying samples having different initial states of strain hardening and iron and silicon contents using thermoelectric power as a measurement technique. By determining the time-temperature-transformation diagrams, they concluded that iron is the alloying addition that controls the precipitation kinetics of the material. Microstructural changes during the annealing of AA8011 foils have been studied by Oscarson *et al*. [2]. They showed that there is a transition for normal discontinuous recrystallization towards continuous recrystallization as the level of deformation increases. The influence of microstructure and texture on the earing behavior of the material has been investigated by Anderson *et al*. [3]. The alloys with different amounts of Si and Fe were characterized in terms of the size distributions of second phase precipitates and elements in solid solution.

Forming limit diagrams of AA8011 sheets has been calculated using Hosford's yield criterion and different hardening laws by Aghaie-Khafri [4]. However, there is a lack of comprehensive investigations on the relation between forming behavior and microstructure of the material under different annealing and homogenization conditions. The FLD is a useful diagnostic tool for trouble shooting in sheet metal formability operations and is also an assessment method for determining the formability of different sheet materials [5, 6]. The level and shape of the FLD's are affected strongly by the strain hardening and strain-rate sensitivity parameters of the material. Furthermore, to obtain a better explanation of experimental data, various aspects of the microstructure like surface roughness and texture should also be considered as effective parameters [7, 8].

Homogenization of as cast material have an impact on the subsequent processability, and influence the final product properties [9, 10]. The present investigation examines the influence of homogenization on the uniaxial and biaxial deformation behavior of the roll-cast AA8011 aluminum alloy sheets.

2. Experimental procedures

2.1. Materials and processing

The material used in this investigation was an aluminum-rich eutectic alloy AA8011 containing (in wt%) 0.83 Fe, 0.59 Si with minor constituents of 0.025 Mn, 0.01 Cu, 0.05 Zn and 0.02 Ti. It was roll-cast to 8 mm thickness before receiving different thermomechanical treatments. Some of the strips were cold rolled to a final thickness of 0.9 mm without prior homogenization, and some others were homogenized at 560°C for eight hours, furnace cooled, and then cold rolled to the same final thickness. In both conditions the rolled sheets were annealed in the temperature range of 280–450°C. Homogenized and unhomogenized conditions are referred to hereafter as "H" and "U" respectively, followed by the annealing temperature.

2.2. Uniaxial tensile tests

Uniaxial tensile test specimens, 75 mm long and 12 mm wide prepared from the sheets at 0, 45 and 90°to the rolling direction, were pulled to fracture at a cross-head speed of 5 mm min^{-1}, producing an average strain rate of $1 \times 10^{-3}s^{-1}$ as the specimen extended. Load-extension curves were obtained with the aid of a 25 mm gauge length extensometer, from which the nominal and true stress-strain curves were calculated. The true stress-true strain data in the uniform straining range were fitted to the Hollomon equation ($\sigma = k\varepsilon^{n}$) from which, hardening parameters were obtained using a least-squares method. Computer software were used to calculate the slope of true stress-true strain curve at different points and uniform strain were obtained numerically from the intersection of $d\sigma/d\varepsilon$ and σ curves. The instantaneous strain-rate sensitivity index, m, was determined using step changes in cross-head speed, from $v_1 = 5$ to $v_2 = 50$ mm min^{-1} which produced strain-rates of $\dot{\varepsilon}_1 = 1 \times 10^{-3}s^{-1}$ to $\dot{\varepsilon}_2 = 10 \times 10^{-3}s^{-1}$. Using extrapolation procedure two stresses, σ_1 and σ_2, are compared at the same strain and the m value was obtained from $m = \frac{\ln(\sigma_2/\sigma_1)}{\ln(\dot{\varepsilon}_2/\dot{\varepsilon}_1)}$. All mechanical properties (X) were average values calculated from the following equation:

$$X_{ave} = \frac{X_0 + 2X_{45} + X_{90}}{4} \quad (1)$$

where 0, 45 and 90 refer to the direction of the specimens to the rolling direction.

2.3. Limit strain measurements

Rectangular strips of varying width were cut from the sheets with the long dimension of the rectangle parallel to rolling direction. After annealing, a circular grid pattern with a circle diameter of 2 mm was etched onto the surface of each test-piece. The strips were then stretched over a 50 mm diameter hemispherical punch until they fractured, using polyethylene film as a lubricant. Surface strains were determined by measuring the major and minor diameters of the ellipses. The closest unfractured ellipses to the cracks were considered to embrace "necking" strains, and other ellipses were defined as "safe" strains, shown schematically in Fig. 1. Forming limit diagrams were then drawn above the safe ellipses and below the necked ones.

2.4. Surface roughness measurements

Surface roughness of sheets strained up to the onset of necking (maximum uniform strain) was measured using a Mititoyo surface texture measuring system. The measurement conditions were as follows: traveling length, 5 mm; cut-off length, 0.8 mm; tracing speed of stylus, 0.5 mm s^{-1}. Direct measurements of surface roughness and waviness were made from a single traverse over the surface, both being recorded on a profile graph. Other traverses parallel to the first trace were attempted to ensure the consistency and uniformity of the results. To accommodate the profile variations, the arithmetic mean value, R_a, was employed as the roughness parameter in this work.

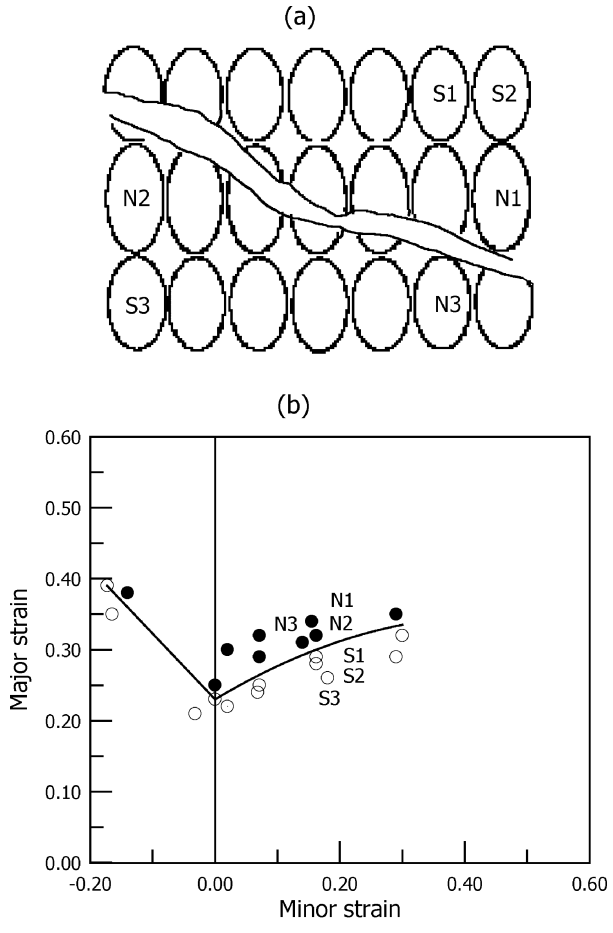

Figure 1 Schematic representation of the printed circles near a localized neck (a), and a plot of the strains in the deformed circles (b). Solid points represent the circles through which necking has occurred (N) and open circles show the unfractured or safe (S) circles. Forming limit curves are drawn above the safe ellipses and below the necked ones.

3. Results and discussion

Nominal stress-strain curves corresponding to an average strain rate of $1 \times 10^{-3}s^{-1}$, obtained for the homogenized and unhomogenized conditions annealed at various temperatures, are shown in Fig. 2. As shown in this figure, different conditions of the material showed different behavior in terms of flow stress and elongation. The curves for the recrystallized conditions show significant plastic deformation before fracture, while for the low annealing temperature conditions (U280 and H280), with predominantly recovered structures, the stress-strain curves exhibit premature failure.

Material parameters such as strain-hardening exponent, n, strain-rate sensitivity index, m, for different heat treatments are listed in Table I. It can be observed that the strain-hardening exponents in both conditions

TABLE I Summary of mechanical characteristics for sheets in the unhomogenized and homogenized conditions

Annealing	Unhomogenized			Homogenized		
temperature (°C)	n	ε_u	m	n	ε_u	m
280	0.045	0.038	0.003	0.070	0.050	0.002
350	0.225	0.182	0.002	0.270	0.224	0.001
450	0.280	0.226	0.001	0.293	0.194	0.000

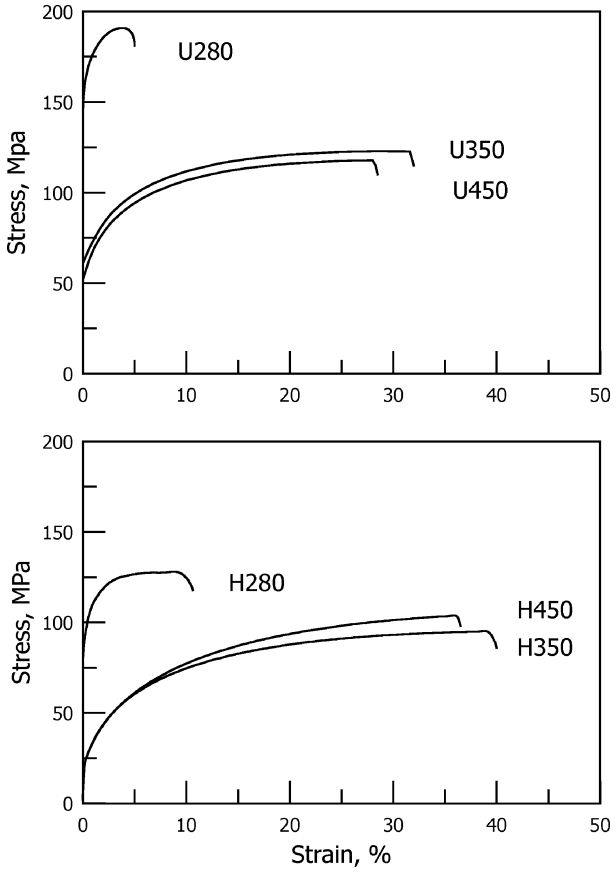

Figure 2 Engineering stress-strain curves for the unhomogenized and homogenized sheets annealed at different temperatures.

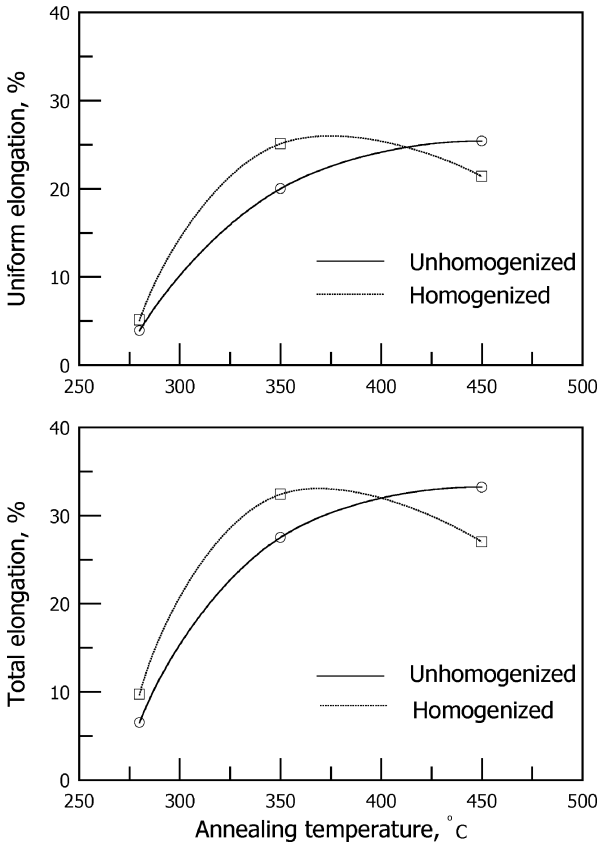

Figure 3 Variation of uniform and total elongation with annealing temperature for unhomogenized and homogenized conditions.

increased with increasing annealing temperature. This will in turn improve the formability of the material through its influence on the materials ability to distribute strain more uniformly. On the other hand, strain-rate sensitivity index tends to decrease with increasing annealing temperature. The high-temperature homogenization treatment has resulted in annealed structures with coarser grains which obviously provide nonuniform deformation.

The uniform deformation is calculated based on Considére criterion which is an upper limit, and assumes homogeneous deformation up to the initiation of a geometrical instability. The variation of uniform and total elongations with annealing temperature for homogenized and unhomogenized conditions are shown in Fig. 3. It is clear that both uniform and total elongations of the unhomogenized sheets increased with increasing annealing temperature. For the homogenized materials, however, there existed a critical annealing temperature above which, both of the elongation values showed a decreasing pattern.

Figs 4 and 5 show the forming limit diagrams of the unhomogenized and homogenized sheets annealed at different temperatures. As shown in these figures, the high temperature annealing treatments developed high limit strains throughout the biaxial stretching regime. The measured rate-sensitivities (Table I) showed that m-values of the U280 and H280 materials were typically higher than those of the sheets annealed at higher temperatures. However, For m values to have an influence on neck growth rates values of greater than 0.01

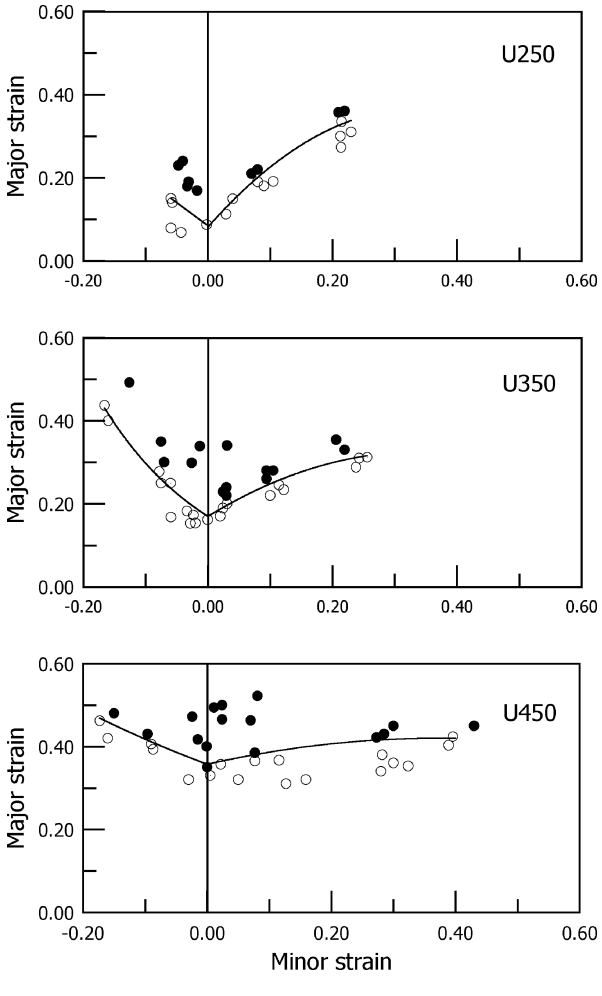

Figure 4 Forming limit diagrams of the unhomogenized sheets, where solid and hollow circles represent neck and safe strains, respectively.

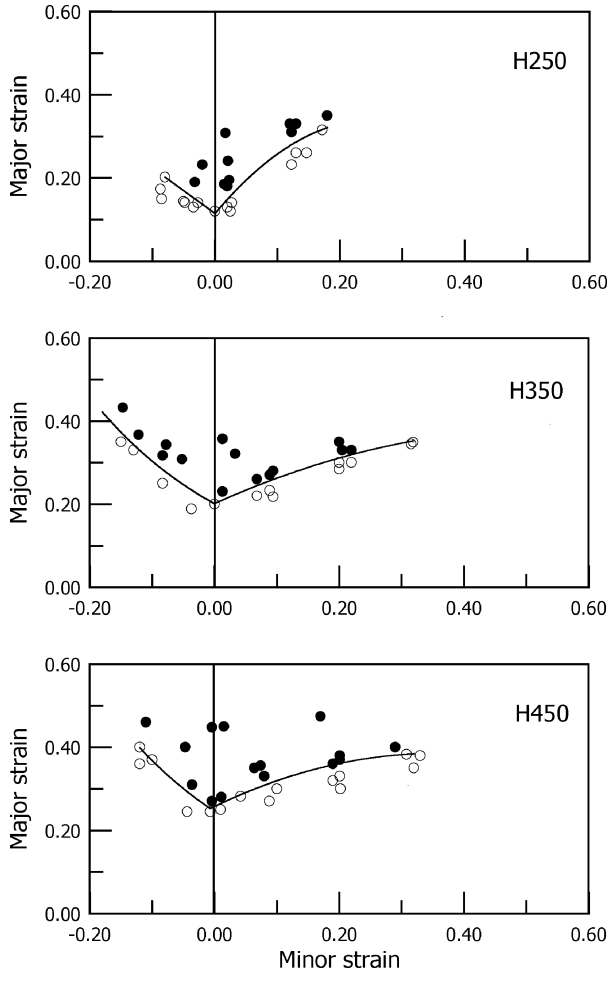

Figure 5 Forming limit diagram of the homogenized sheets, where solid and hollow circles represent neck and safe strains, respectively.

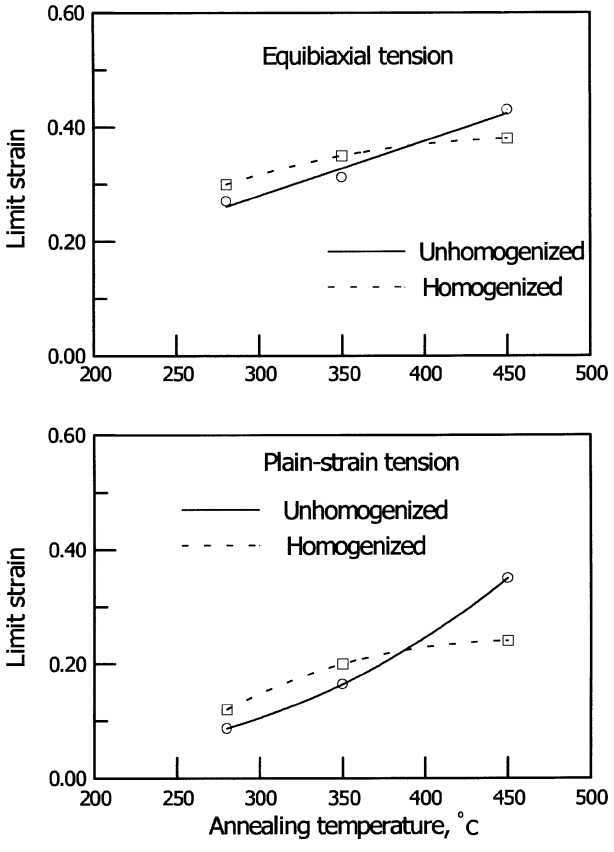

Figure 6 Variation of limit strains with annealing temperature for unhomogenized and homogenized sheets under equibiaxial and plane-strain conditions.

are typically required [11]. Therefore, the main cause of the superior limit strains of the recrystallized sheets appear to be their higher n-values, microstructural refinement and uniformity.

The curves for the recrystallized conditions show significant negative and positive minor straining, resulting in relatively wide forming limit diagrams. However, for the low annealing temperature conditions (U280 and H280) the FLDs are limited and steep. Based on the experimental FLDs obtained, limit strains for the plane-strain and equibiaxial states are plotted against the annealing temperature (Fig. 6). It can be seen that although in both cases the limit strains increased with increasing annealing temperature, the curves show different trends for different heat treatments. It is clear that before a critical annealing temperature homogenized sheets show superior formability, but formability is reduced beyond this critical temperature.

The results of surface roughness measurements are shown in Fig. 7. It is clear that surface roughness increased with increasing annealing temperature, being always higher for the homogenized conditions. Furthermore, both uniaxial and biaxial formability of homogenized sheets showed a decreasing pattern close to the temperature that above which surface roughness in homogenized condition significantly increased. Surface roughness is a reflection of the slip events that occur during deformation leading to necking and subsequent

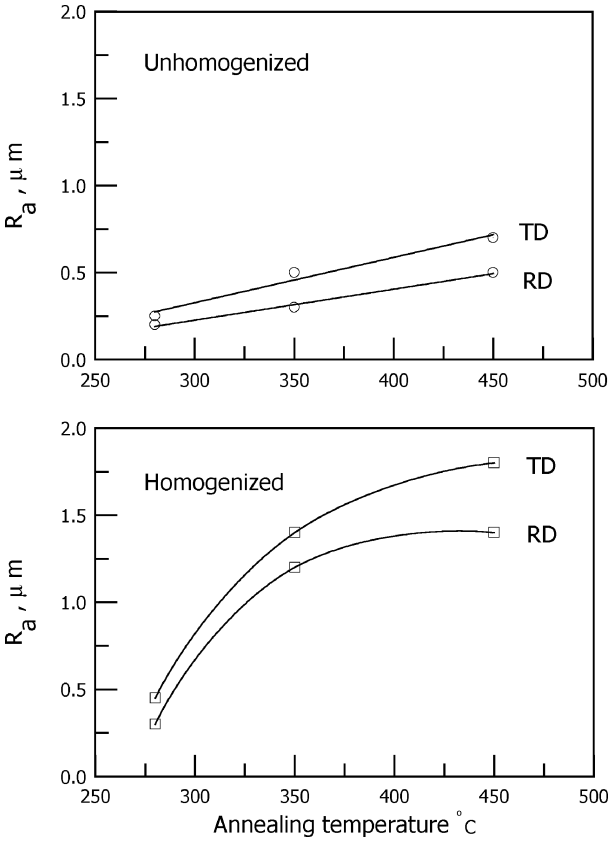

Figure 7 Variation of roughness with annealing temperature for unhomogenized and homogenized sheets in the rolling and transverse directions.

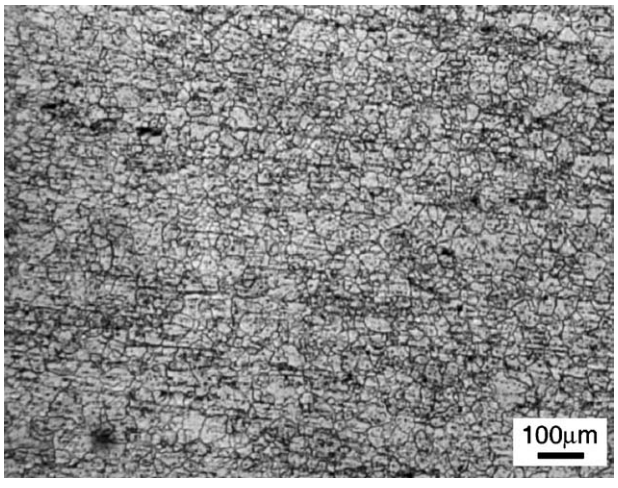

Figure 8 Optical micrograph of homogenized sheet following annealing at 450°C.

failure at large strains. Several workers have studied the evolution of surface roughness in plane stretching as well as during punch stretching process, and have emphasized its role in the onset of macroscopic flow localization [7]. As a result, it can be postulated that different roughness behavior of material in homogenized and unhomogenized conditions might be a dominant parameter that can affect the formability of the AA8011 aluminum alloy.

Yamaguchi and Mellor [12] investigated the roughness under biaxial stretching and showed that the roughness of material was proportional to the magnitude of the equivalent strain and the grain size. At low annealing temperature the material had, recovered or fine recrystallized structure, in this case roughness is not a dominant parameter, therefore homogenized materials which have greater n values show higher strain levels. However, after high annealing temperature the homogenized sheets show inferior formability due mainly to the grain size of the homogenized materials (Fig. 8), which were typically coarser than those of unhomogenized sheets resulted in higher values of surface roughness.

The process of recrystallization and therefore the grain sizes in homogenized and unhomogenized conditions is influenced by the presence of a dispersion

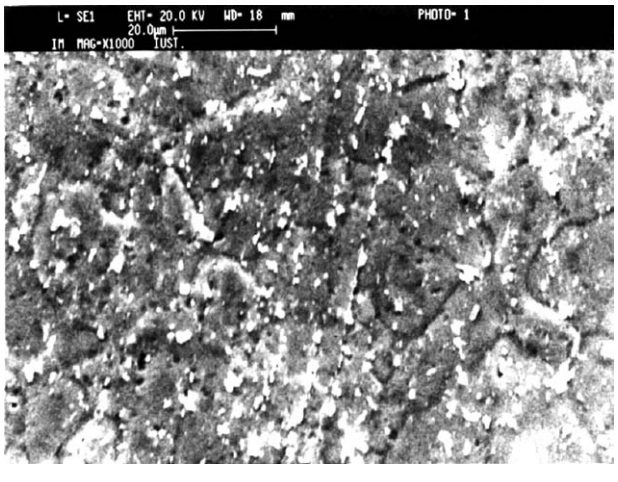

Figure 9 SEM micrograph of second phase particles in unhomogenized sheet following annealing at 450°C.

TABLE II Particle size, particle volume fraction and Zener pinning force measured at different annealing temperatures

Annealing temperature (°C)	Unhomogenized			Homogenized		
	d (μm)	F_v	P_z (MN/m^2)	d (μm)	F_v	P_z (MN/m^2)
280	0.30	0.041	0.26	0.72	0.072	0.19
350	0.70	0.052	0.14	1.34	0.075	0.10
450	1.00	0.071	0.13	1.88	0.081	0.08

of second-phase particles in the deformed matrix [13]. The AA8011 material contains a distribution of both large and small particles ranges between 0.3 and 1 μm as shown in Fig. 9. Based on image analysis data (Table II) the pinning forces due to particles were calculated using the Zener pinning equation for a random distribution of spherical particles

$$P_Z = \frac{3F_V\gamma_B}{2r}$$

where F_V is the particle volume fraction, r the particle radius and γ_B the grain boundary energy. For aluminum, taking the energy of a high-angle grain boundary to be 0.625 J/m^2 [14], the pinning force exerted at each annealing temperature was calculated and is given in Table II. If the Zener pinning force is plotted as a function of annealing temperature (Fig. 10) it is apparent that the pinning force is smaller for homogenized condition resulting in greater grain sizes. The limiting grain sizes at different annealing temperature can be approximated using the Zener limit equation [13]:

$$D_Z = k\left(\frac{r}{F_V}\right)$$

Moreover, there is a good correlation of surface roughness and uniform strain with $\frac{r}{F_V}$ shown in Fig. 11. Consequently, we may consider $\frac{r}{F_V}$ as a formability parameter that influence the ductility of AA8011 in homogenized condition.

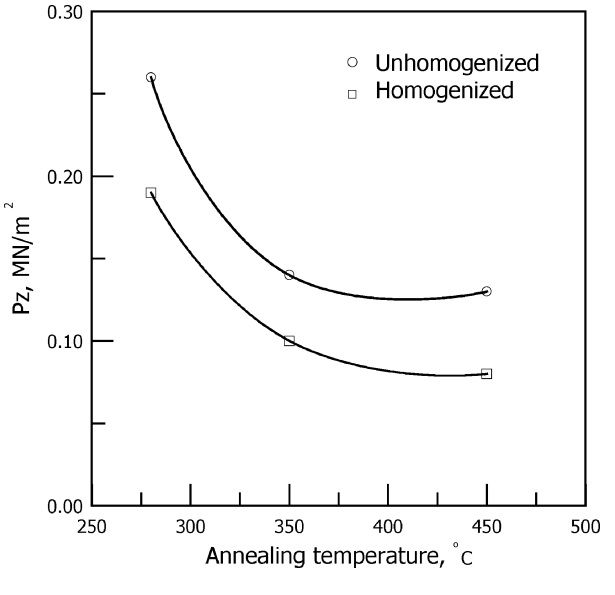

Figure 10 Graph showing the relationship between Zener pinning force and annealing temperature.

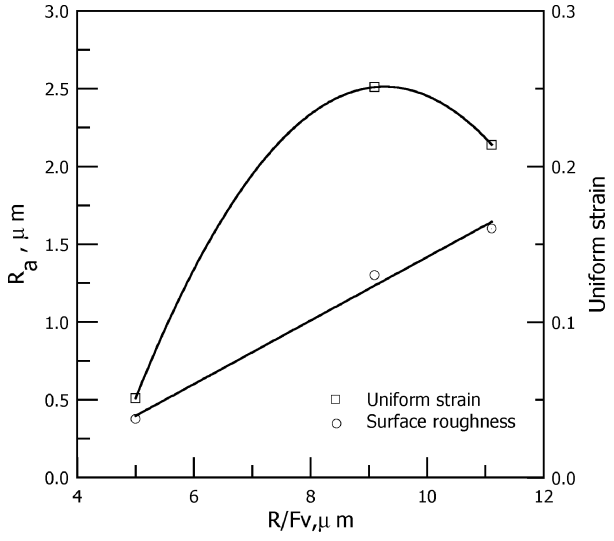

Figure 11 Variation of roughness and uniform strain with $\frac{r}{Fv}$ for homogenized sheets.

Finally, it is concluded that the major difference between homogenized and non-homogenized material is that the elevated temperature treatment removes short wavelength solute segregation, and depending on the thermal history associated with the homogenization treatment, precipitates Fe and Si from solution. Fe and Si in solution controls work hardening behavior in this alloy. Moreover, homogenization of as cast material brings about changes in size, shape and distribution of primary and secondary precipitates which in turn, impact the subsequent recrystallization process and influence the final product properties such as strength and formability.

4. Conclusions

The stretch formability of AA8011 aluminum alloy, as indicated by forming limit diagrams and uniaxial fracture strains, is affected strongly by the strain hardening, strain-rate hardening and surface roughness of the material. Strain hardening and strain rate-hardening are expected to be the dominant factors in determining the formability of unhomogenized sheets, while surface roughness is believed to decrease the forming limits of the homogenized materials. Despite the higher formability of the homogenized sheets at low annealing temperature, their biaxial stretch-ability was found to be inferior to those of the unhomogenized material at high annealing temperatures. This could have been caused by the grain coarsening effect, which is in turn a result of low Zener pinning force in homogenized sheets. This effect encourages the surface roughening which can adversely affect the biaxial stretch-ability of the material in this condition.

References

1. J. NEY and A. LUIGGI, *Metall. Mater. Trans.* **19A** (1998) 2669.
2. A. OSCARSON, B. LEHTINEN, B. HUTCHINSON, H. E. EKSTRON, P. BATE, L. HAGGSTRON and A. M. GHANDOUR, in Proceedings of the 4th International Conference on Aluminum Alloys, Atlanta, Georgia, USA (1994) Vol. III, p.144.
3. B. ANDERSON and S. E. NAESS, in Proceedings of the 8th International Light Metals Congress, Leoben-Viena (Aluminium-Verlag GmbH, 1987) p. 526.
4. M. AGHAIE-KHAFRI, R. MAHMUDI and H. PISHBIN, *Metall. Mater. Trans.* **33A** (2002) 1363.
5. E. ROMHANJI, M. OPOVIC, D. GLIS and V. MILENKOVIC, *J. Mater. Sci.* **33** (1998) 1037.
6. M. AGHAIE-KHAFRI and R. MAHMUDI, *Aluminum* **74** (1998) 753.
7. M. JAIN, D. J. LLOYD and S. R. MACEWEN, *Int. J. Mech. Sci.* **38** (1996) 219.
8. L. S. TOTH, J. HIRSCH and P. V. HOUTTLE, *ibid.* **38** (1996) 1117.
9. H. TANIHATA, T. SUGAWARA, K. MATSUDA and S. IKENO, *J. Mater. Sci.* **34** (1999) 1205.
10. M. AGHAIE-KHAFRI and R. MAHMUDI, *JOM* Nov. (1998) 52.
11. A. K. GHOSH, *J. Eng. Mater. Technol. Trans. ASME* **99H** (1977) 264.
12. R. YAMAGUCHI and P. B. MELLOR, *Int. J. Mech. Sci.* **18** (1976) 85.
13. F. J. HUMPHREYS, "Recrystallization and Related Annealing Phenomena" (Pergamon Press, Oxford, 1995).
14. R. K. DAVIES, V. RANDLE and G. J. MARSHALL, *Acta Mater.* **46** (1998) 6021.

Received 1 October 2003
and accepted 23 June 2004